Biophysical Journal
Article

Biophysical Society

Angular Precision of Radical Pair Compass Magnetoreceptors

Yi Ren,[1] Hamish G. Hiscock,[2] and P. J. Hore[1,*]
[1]Department of Chemistry, University of Oxford, Oxford, United Kingdom and [2]Department of Chemistry, Massachusetts Institute of Technology, Cambridge, Massachusetts

ABSTRACT The light-dependent magnetic compass sense of night-migratory songbirds is thought to rely on magnetically sensitive chemical reactions of radical pairs in cryptochrome proteins located in the birds' eyes. Recently, an information theory approach was developed that provides a strict lower bound on the precision with which a bird could estimate its head direction using only geomagnetic cues and a cryptochrome-based radical pair sensor. By means of this lower bound, we show here how the performance of the compass sense could be optimized by adjusting the orientation of cryptochrome molecules within photoreceptor cells, the distribution of cells around the retina, and the effects of the geomagnetic field on the photochemistry of the radical pair.

SIGNIFICANCE Although it has been known for 50 years that small night-migratory songbirds have a light-dependent magnetic compass sense to help them navigate thousands of kilometers every year, the biophysical mechanism remains largely unknown. The leading hypothesis is that the Earth's magnetic field can alter the course of photochemical reactions in the birds' eyes even though the energies involved are a million times smaller than the thermal energy, k_BT. Our results indicate how the precision of this compass could be optimized to make the best use of the relatively small number of photons available to these nocturnal migrants.

INTRODUCTION

Night-migratory songbirds have a light-dependent magnetic compass sense that helps them navigate the thousands of kilometers that separate their breeding and wintering grounds (1–3). How this compass works is something of a mystery (4). Currently, the leading hypothesis for the primary detection event involves the photochemical production of transient radical pairs in cryptochrome proteins contained in the birds' retinas (5–7). The spin dynamics of these paramagnetic reaction intermediates could provide a mechanism by which the direction of the Earth's magnetic field (~50 μT) is encoded in the quantum yield of a signaling state of the protein.

Light is a crucial component of this hypothesis (8,9). Blue light is required to excite the flavin chromophore and trigger the intraprotein electron transfers that generate the radical pairs (5). A fundamental question, therefore, is whether this mechanism is viable given the dim light conditions experienced by nocturnal migrants. This issue has recently been addressed by Hiscock et al. (10), who used an information theory approach to obtain a strict lower bound on the angular precision with which a bird could orient itself using a cryptochrome-based radical pair sensor. The method has the advantage that it avoids having to make guesses about the nature and efficiency of signal transduction and postprocessing in vivo, instead calculating the best-case precision. It was concluded that the average photon flux on a cloudless and moonless night (~3×10^{-4} lux (11)) might not be sufficient for at least some of the currently considered radical pair models.

In this work, we extend this analysis and attempt to answer four main questions. 1) How does the angular precision of a radical pair compass depend on the total number of photons absorbed per second by cryptochromes in the eye? 2) Can the precision of such a compass be improved by optimizing the orientation of the proteins inside photoreceptor cells in the retina? 3) Could the angular precision be increased by concentrating the cells that contain

Submitted October 16, 2020, and accepted for publication December 30, 2020.

*Correspondence: peter.hore@chem.ox.ac.uk

Editor: Alexander Berezhkovskii.
https://doi.org/10.1016/j.bpj.2020.12.023

magnetoreceptors in certain regions of the retina? 4) How does the angular precision depend on the magnetic and kinetic properties of the radicals?

METHODS

Eye model

Following Hiscock et al. (10) and Lau et al. (12), we model the bird's eye as a sphere comprising a hemispherical retina and a pupil positioned diametrically opposite its center (Fig. 1 *a*). Cylindrical receptor cells are distributed around the retina with their symmetry axes pointing toward the center of the sphere. Their locations are specified by angles κ (co-latitude) and ν (azimuth), with $\kappa = 0$ at the center of the retina and $\kappa = 90^\circ$ at its periphery (Fig. 1 *b*). The optical axis of the eye is constrained to the horizontal plane. The direction of the geomagnetic field inside a given cell is therefore determined by κ and ν and by the direction of the optical axis, referred to as the "head direction," θ (Fig. 1 *b*). Although a crude approximation to reality, this geometry captures the essential physics.

There could be more than a million cells in the retina containing magnetoreceptor molecules—far too many to model explicitly (10). To reduce the computational burden, Hiscock et al. treated clusters of neighboring cells, referred to as grouped receptor cells, each of which absorbs the total number of photons that would have been absorbed by the individual cells in the cluster in a given time interval (10). The assumption here is that the cells within a group are sufficiently close together that they have almost identical orientations and therefore very similar responses to the geomagnetic field (13). The number of these groups of cells is denoted r. Hiscock et al. generated a 180×180 square grid of points on a plane tangent to the center of the retina, which was then mapped onto the retina by means of a stereographic projection using the pupil as the point of perspective (10). The result was an array of 25,132 grouped cells covering the whole retina. As we shall see below, accurate estimates of the head direction error can in fact be obtained with far fewer grouped cells. To avoid the higher-than-average density of cells near the edges of the retina resulting from the stereographic projection, we distribute cells here using the SpherePoints function in Mathematica (14), which places points on the surface of a sphere so that they are approximately equally spaced. In practice, this change was found to make little difference to the calculated head direction errors provided $r > 100$. Every grouped cell is assumed to absorb the same number of photons per second irrespective of both the head direction and the position of the cell in the retina. Every photon absorbed is assumed to give rise to a radical pair. All the cells and their contents are assumed to be identical. The signal from each receptor cell is an average over the radical pairs within it.

Receptor molecules

The radical pair model of compass magnetoreception is based on the formation of light-induced radical pairs in aligned receptor molecules, generally assumed to be cryptochrome proteins, contained in cells in the retina (6,12). The response of a cell to the geomagnetic field is encoded in the yield of a signaling state of the protein produced by chemical reactions of these radical pairs (15). The amplitude of this signal, given the symbol Φ_S, depends on the direction of the magnetic field with respect to the proteins which are assumed to have identical intracellular orientations. The direction of the geomagnetic field with respect to the receptor molecules is therefore completely determined by θ (the head direction), by ν and κ (the position of the cell in the eye), and by the orientation of the proteins within the cell.

We base the calculations here on a model of the [$FAD^{\bullet-}$ $TrpH^{\bullet+}$] radical pair formed in cryptochrome by electron transfer along a triad or tetrad of tryptophan (TrpH) residues to the photoexcited singlet state of the noncovalently bound flavin adenine dinucleotide (FAD) chromophore. Although magnetic field effects have been reported for a few purified cryptochromes and are generated by [$FAD^{\bullet-}$ $TrpH^{\bullet+}$] radical pairs (16,17), it has not yet been possible to measure the dependence of the quantum yield of a potential signaling state on the direction of an external magnetic field. Following Hiscock et al. (10), we therefore base these calculations on spin dynamics simulations of [$FAD^{\bullet-}$ $TrpH^{\bullet+}$]. Previous work has shown that Φ_S is dominated by the axial hyperfine interactions of two nitrogen nuclei in $FAD^{\bullet-}$ (18,19) such that Φ_S has an approximately axial symmetry around the normal to the plane of the isoalloxazine group of the flavin (denoted the z axis). The anisotropy of Φ_S is therefore determined by the angle, ζ, between the flavin z axis and the direction of the geomagnetic field experienced by the radical pair. We assume perfect axial symmetry here. As a result, only two angles are required to specify the orientation of the cryptochrome molecules within a cell: the co-latitude, β, and the azimuth, α. When $\beta = 0$, the magnetic symmetry axis of the flavin ring system in a cryptochrome molecule is parallel to the symmetry axis of the cell that contains it, and the cell axis points toward the center of the eye. Fig. 1 *c* shows the three molecular orientations considered below: O1 ($\beta = \pi/2$, $\alpha = \pi/2$), O2 ($\beta = \pi/2$, $\alpha = 0$), and O3 ($\beta = 0$).

Following Hiscock et al. (10), we use a simple parameterized model of the dependence of the yield of the signaling state on ζ:

$$\Phi_S(\zeta) = a - b \exp\left[\frac{(\zeta - 90^\circ)^2}{2c^2}\right]. \qquad (1)$$

This form of $\Phi_S(\zeta)$ is an inverted Gaussian, centered at $\zeta = 90^\circ$, with offset a, amplitude b, and half-width c and default values $a = 0.5$, $b =$

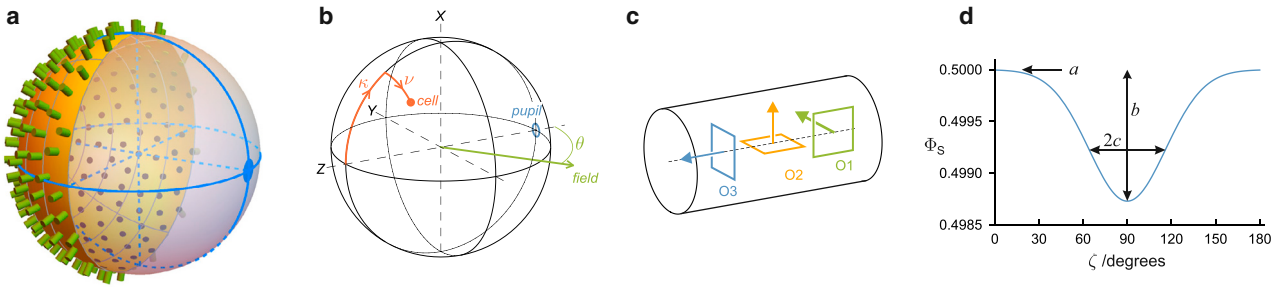

FIGURE 1 (*a*) A representation of the model eye used to estimate the precision with which radical pair magnetoreceptors can provide a compass bearing. Cylindrical receptor cells (*green*) are distributed uniformly around the hemispherical retina (*orange*), whose center is diametrically opposite the pupil (*blue disk*). (*b*) The positions of cells within the retina are specified by angles κ (rotation around the y axis, here $+0.3\pi$) and ν (subsequent rotation around the z axis, here -0.2π). θ, the head direction, is the angle between the optical axis and the horizontal component of the geomagnetic field. (*c*) Orientations O1–O3 of the cryptochromes within a cylindrical cell are shown. The arrows indicate the magnetic symmetry (z) axis of the flavin. (*d*) The default model signal, Eq. 1, is shown with $a = 0.5$, $b = 0.00127$, and $c = 26^\circ$.

0.00127, and $c = 26°$ (Fig. 1 *d*). When $\zeta = 90°$, the magnetic field is perpendicular to the z axis of the flavin. These numbers were chosen (10) to give an approximate match to a quantum spin dynamics simulation of Φ_S for a model of [$FAD^{\bullet-}$ $TrpH^{\bullet+}$] containing seven nuclear spins in each radical, no electron-electron exchange or dipolar couplings, and a 1 μs lifetime. A more detailed simulation of [$FAD^{\bullet-}$ $TrpH^{\bullet+}$] including exchange and dipolar interactions with a total of 27 nuclear spins (20) gave a smaller value of the amplitude b (10). Larger values of b were obtained when the lifetime was increased to 5 μs or when $TrpH^{\bullet+}$ was replaced by either an ascorbyl radical or a hypothetical radical with no hyperfine interactions (10).

For the three intracellular orientations O1, O2, and O3 (Fig. 1 *c*), straightforward geometry gives the following expressions for ζ in a cell with position (ν, κ) in an eye with head direction θ (Supporting Materials and Methods):

$$\mathrm{O1}: \cos\zeta = \sin\phi\sin\nu + \cos\phi\sin\theta\cos\nu, \tag{2}$$

$$\mathrm{O2}: \cos\zeta = -\cos\nu\cos\kappa\sin\phi + \cos\phi\cos\kappa\sin\nu\sin\theta + \cos\phi\cos\theta\sin\kappa, \tag{3}$$

and

$$\mathrm{O3}: \cos\zeta = -\cos\phi\cos\theta\cos\kappa - \cos\nu\sin\phi\sin\kappa + \cos\phi\sin\nu\sin\theta\sin\kappa. \tag{4}$$

The angle ϕ (taken to be 66°) is the geomagnetic inclination. Hiscock et al. considered only the orientation O1, for which $\cos\zeta$ has a simpler dependence on the position of the cells in the retina, being a function of ν but not κ (10).

Information theory

The signaling pathway can be represented by the sequence input → encoding → decoding → output. In general, encoding involves some loss of information that cannot be restored by the decoder, resulting in the output being an imperfect reflection of the input. Results from rate distortion theory (21,22), the branch of information theory (23–26) concerned with lossy data compression, allow us to determine a lower bound on the uncertainty in the output. Returning to magnetoreception, the input is the direction of the geomagnetic field relative to the bird's head direction. This information is encoded in the yields of the radical pair reactions of the cryptochromes contained in cells in the retina. The signal produced by a cell is the average of the yields of the reaction cycles of its cryptochromes. It encodes the direction of the geomagnetic field within the cell via the position of the cell in the curved retina. The set of signals from the whole retina is then interpreted by some unknown decoding mechanism involving signal transduction and data processing in the eye and the brain. The output of the signaling pathway is an estimate of the bird's head direction relative to the geomagnetic field vector, which can then be integrated in the brain with directional information from other senses. The encoding process is noisy when the number of photons, and therefore the number of radical pairs, is limited because each individual reaction cycle starts with a random nuclear spin configuration and ends with a reaction event with a different timing. Only in the limit of an infinite number of radical pairs is this reaction yield equal to that calculated using master equation methods. The incomplete averaging of this quantum noise degrades the information available from the encoding and leads to an uncertainty in the estimated head direction. In the approach devised by Hiscock et al. (10), our near-complete lack of knowledge of the decoding process is conveniently sidestepped by assuming it to be optimal, i.e., that it retains 100% of the information contained in the noisy reaction yield signals and so leads to the best-case compass precision. For details of the theory, the reader is referred to (10).

Lower bound error in the head direction

Hiscock et al. derived the following expression (a rearranged form of their Eq. S19) for ε_H, the lower bound on the root mean-square error in the head direction estimate obtained from an encoding of the true head direction by molecules in cells distributed around the retina (10):

$$\varepsilon_H = \sqrt{\frac{2\pi}{e}\frac{1}{\det(\boldsymbol{\Sigma})}\exp\left[\sum_{i=1}^{r}\overline{\ln\left(\sigma_{i,\theta}^2\right)}\right]}. \tag{5}$$

We refer to ε_H here as the lower bound error in the head direction. In Eq. 5, $\boldsymbol{\Sigma}$ is the $r \times r$ covariance matrix with elements

$$\Sigma_{ij} = \overline{\left(\Phi_S^{i,\theta}\Phi_S^{j,\theta}\right)} - \left(\overline{\Phi_S^{i,\theta}}\right)\left(\overline{\Phi_S^{j,\theta}}\right) + \delta_{ij}\overline{\sigma_{i,\theta}^2}, \tag{6}$$

in which $\Phi_S^{i,\theta}$ is the signal for cell i and head direction θ, δ_{ij} is the Kronecker δ, and

$$\sigma_{i,\theta}^2 = \frac{1}{p}\Phi_S^{i,\theta}\left(1 - \Phi_S^{i,\theta}\right), \tag{7}$$

with p the number of photons absorbed per grouped receptor cell in a certain time interval. The overbars indicate an average over all head directions ($0 \le \theta < 2\pi$) in the horizontal plane.

The fundamental quantity on which Eq. 5 is based is the mutual information between the actual head direction and the estimated head direction. This is a measure of how much uncertainty there is in the output of the information channel for a given input (26). This is obviously impractical to calculate, and so we use the data processing inequality (27,28) to place an upper bound on the mutual information (which translates into a lower bound in the error in the head direction estimate). The assumption invoked in using this relation is that the sole source of magnetic information available to the bird is contained within the reaction yield signal and that the estimate of the head direction relative to an external magnetic field is constructed using only this information. The signaling pathway therefore forms a Markov chain, and the maximal possible information available at the output is equal to the information contained in the encoded input, i.e., the total information contained in the reaction yield signal.

This mutual information can be related to the lower bound heading error through the Shannon entropy (23) of the head direction estimate, which is the formal quantity in the context of information theory that measures uncertainty in a variable. Because this entropy is bounded by a closed form expression in terms of the variance of the variable distribution, after some manipulations (10) we can come to an expression for ε_H in terms of the mutual information between the head direction and the singlet yield signal. On substituting expressions to calculate the mutual information (Supporting Material of (10)), we arrive at Eq. 5.

To summarize, the following steps are required to calculate ε_H for a given choice of $\Phi_S(\zeta)$, r, p, and receptor orientation: 1) determine κ and ν for each of the r receptor cells. 2) Calculate $\cos\zeta$ (Eqs. 2, 3, or 4) and hence $\Phi_S(\zeta)$ (Eq. 1) for each cell for each of $K = 1000$ equally spaced values of θ between 0 and 2π. 3) Obtain $\left(\Phi_S^{i,\theta}\right)$, $\left(\Phi_S^{i,\theta}\Phi_S^{j,\theta}\right)$, and $\ln(\sigma_{i,\theta}^2)$ by averaging over θ. 4) Use Eqs. 5, 6, and 7 to compute ε_H. Numerical errors arising from very small values of both $\det(\boldsymbol{\Sigma})$ and the exponential term in Eq. 5 can be avoided by multiplying all elements of $\boldsymbol{\Sigma}$ by $s = (a(1-a))^{-1}$ and adding $r\ln(s)$ to the argument of the exponential in Eq. 5, where a is the offset in the model signal (Eq. 1).

Migratory songbirds can detect the axis of the geomagnetic field with an accuracy better than 5° (29,30). For the purposes of this work, we consider as viable a model compass for which $\varepsilon_H < 5°$.

RESULTS AND DISCUSSION

Dependence of ε_H on total number of photons

The precision with which radical-pair-based sensors can determine a magnetic compass bearing should improve as either the number of receptor cells, r, or the number of photons absorbed by each cell, p, is increased. To explore this dependence in more detail, we calculated ε_H for a range of values of r and p using the default model signal in Eq. 1 and a uniform distribution of cells across the retina. Fig. 2 shows ε_H for orientation O1 as a function of r for four values of the product rp. Similar results were found for orientations O2 and O3 (Fig. S1). Provided $r > 100$, ε_H is independent of r for a fixed value of rp and decreases as rp is increased. That is, when there are more than ~100 grouped receptor cells, the precision of the compass bearing is determined by the total number of photons absorbed across the whole retina, i.e., the total number of photo-induced radical pairs. One of the implications of this finding, which only seems to break down when 1) the offset is outside the range $0.1 < a < 0.9$, 2) the amplitude of the signal is unrealistically large (e.g., $b > 0.1$), or 3) its width is exceedingly narrow (e.g., $c < 0.1°$), is that it is harmless to model large groupings of cells. This finding validates the concept of grouped receptor cells as proposed by Hiscock et al. (10) and greatly reduces the computational burden. The conclusion that rp is the important factor in determining ε_H also holds true for any specified region of the retina as long as the grouped receptor cells are uniformly distributed within that region (Fig. S2).

The total number of photons (rp) impinging on the double cone photoreceptor cells in the eye of a small songbird on a clear moonless night may be estimated as follows: each cell receives ~1 photon per second (5), there is one cell per ~40 μm^2 of retina (31), and the radius of the hemispherical retina is ~4 mm (32). Combining these numbers gives $rp \approx 3 \times 10^6\ s^{-1}$. It seems likely that the signal-to-noise ratio of magnetic sensing could be improved by integrating the signal over a short period of time. An estimate of this time comes from experiments in which birds that had been exposed to eastward-rotated magnetic fields during the twilight period before take-off were observed to fly westward instead of the northerly direction of birds that had experienced the ambient geomagnetic field (11). Quoting Cochran et al., "Our data suggest that the time it takes *Catharus* thrushes to determine a magnetic compass direction while aloft must be relatively short, because we recorded several headings of treated birds within a few minutes after take-off and all of these headings were already deflected" (11). From this, we infer an integration period of no more than ~100 s such that the total number of photons, and therefore radical pairs, required to obtain a compass bearing could be on the order of 3×10^8. As can be seen from Fig. 2, $rp = 3 \times 10^8$ is just about sufficient to achieve a lower bound of 5° when using the default model signal (Eq. 1).

Dependence of ε_H on receptor orientation

Fig. 3 shows ε_H for the three orientations O1–O3 in Eqs. 2, 3, and 4, again using the default parameters for $\Phi_S(\zeta)$ in Eq. 1. All three give $\varepsilon_H = \sqrt{2\pi/e}$ radians = 87.1° in the limit of small rp, dropping down to zero for large rp. For intermediate values of the total number of photons, O2 and O3 give very similar ε_H-values that are significantly smaller than those for O1 for all values of rp between ~10^6 and ~10^9. For example, to achieve a lower bound of 5°, rp must be 2.28×10^8 for O1, 5.26×10^7 for O2, and 5.42×10^7 for O3, i.e., in the ratio

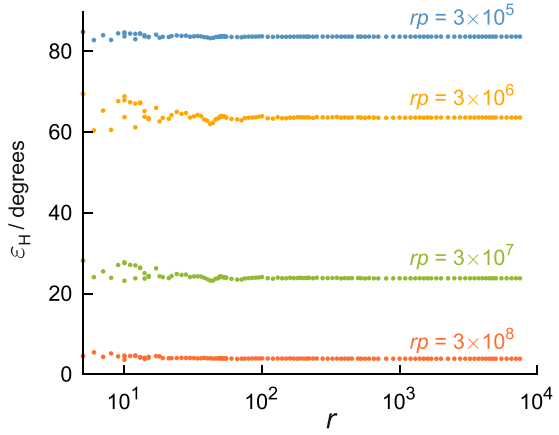

FIGURE 2 Lower bound error calculated using the default model signal (Eq. 1 with $a = 0.5$, $b = 0.00127$, and $c = 26°$), as a function of the number of grouped receptor cells for four values of rp, the total number of photons absorbed across the retina.

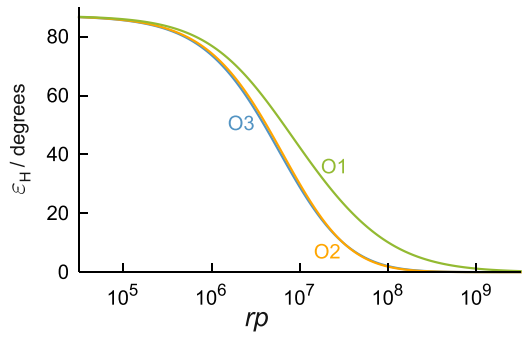

FIGURE 3 Lower bound error as a function of rp for the three orientations, O1–O3, using the default model signal (Eq. 1). The corresponding values of ε_H for O1 shown in Fig. 4, *c* and *e* of Hiscock et al. (10) were calculated using half of the available information (i.e., $-90° < \theta < 90°$) so that artificial processing routines could be used to estimate the attainable heading accuracy. For this reason, the values of ε_H presented here, which use all the available information ($-180° < \theta < 180°$), are larger by a factor of 2.

4.33:1.00:1.03, respectively. O1, which gives the least precise compass bearing, is the orientation chosen by Hiscock et al. to assess the performance of different cryptochrome-based radical pairs (10). It appears that O2 and O3 are very close to optimal. Although we were able to find orientations for which ε_H is slightly smaller than for O2 and O3, this was only possible for values of rp for which the compass is very imprecise (e.g., $\varepsilon_H > 10°$, Fig. S3). Using the default model, we were unable to find an orientation that gave a poorer performance than O1 for any value of rp.

The dependence of ε_H on rp was found to be reasonably well described by the empirical expression

$$\varepsilon_H \approx \sqrt{\frac{2\pi}{e}\left(\frac{1}{1+a_1 rp+(a_2 rp)^2}\right)}. \quad (8)$$

Good agreement with the data in Fig. 3 is obtained with the following values of a_1 and a_2:

$$\begin{aligned} &O1: a_1 = 2.718 \times 10^{-7}, a_2 = 0.659 \times 10^{-7};\\ &O2: a_1 = 3.044 \times 10^{-7}, a_2 = 2.363 \times 10^{-7};\\ &O3: a_1 = 3.208 \times 10^{-7}, a_2 = 2.348 \times 10^{-7}. \end{aligned} \quad (9)$$

Origin of differences between orientations

We have shown above that ε_H is affected by the orientation of the radical pairs within the receptor cells and that O1 performs significantly less well than O2 and O3. Some insight into these differences can be obtained by considering the variation of the signal strength, $\Phi_S(\nu, \kappa)$, across the retina by means of stereographic projections of the retina onto a disk tangent to the center of the retina using the pupil as the point of perspective. When the projected function is $\Phi_S(\nu, \kappa)$, these projections have been called visual modulation patterns (VMPs) (6). Fig. 4 shows VMPs of the default signal for five head directions and the three receptor orientations. In these plots, the dependence of $\Phi_S(\nu, \kappa)$ on κ (co-latitude) and ν (azimuth) is represented, respectively, by radial and angular variations in the VMP. The center of the retina ($\kappa = 0$) projects to the center of the VMP. In all three cases, the pattern changes with head direction, providing information on the horizontal component of the geomagnetic field. Although the patterns are quite different for the three orientations, it certainly is not clear from Fig. 4 why O2 and O3 are better than O1 in terms of providing a precise compass bearing.

The lower bound error generated by a given pattern of receptor cells and a given orientation of radical pairs within

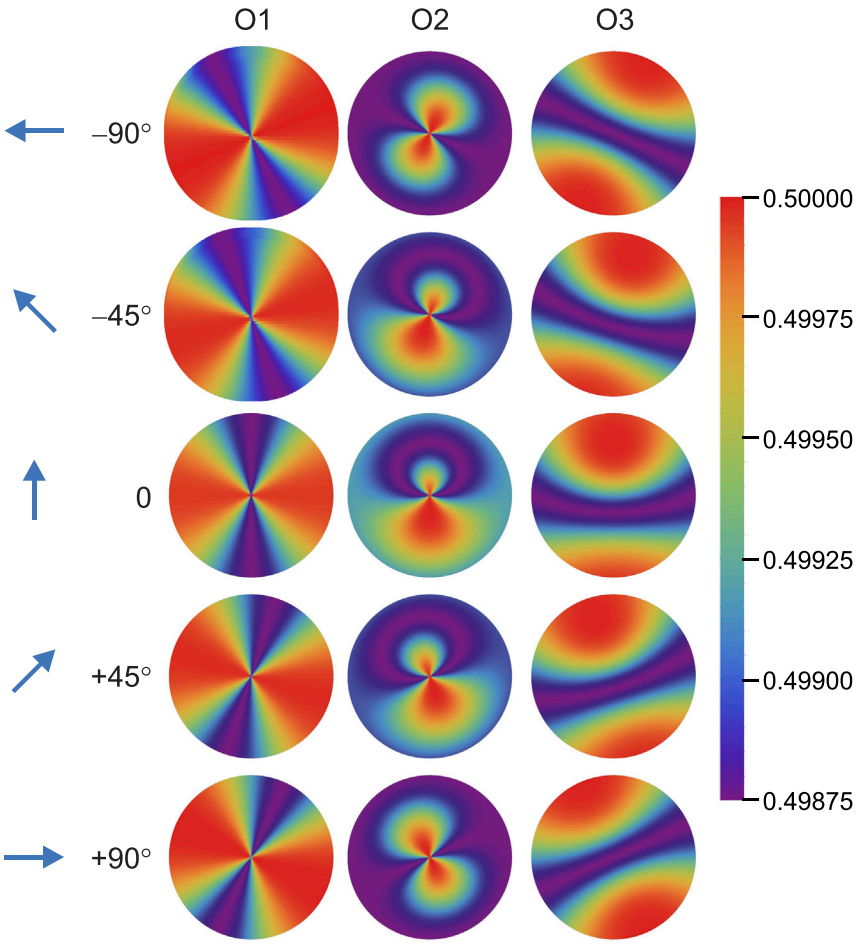

FIGURE 4 VMPs for the default signal $\Phi_S(\nu, \kappa)$ for five head directions, θ, and the three orientations, O1–O3. The arrows and figures on the left show the head direction, θ.

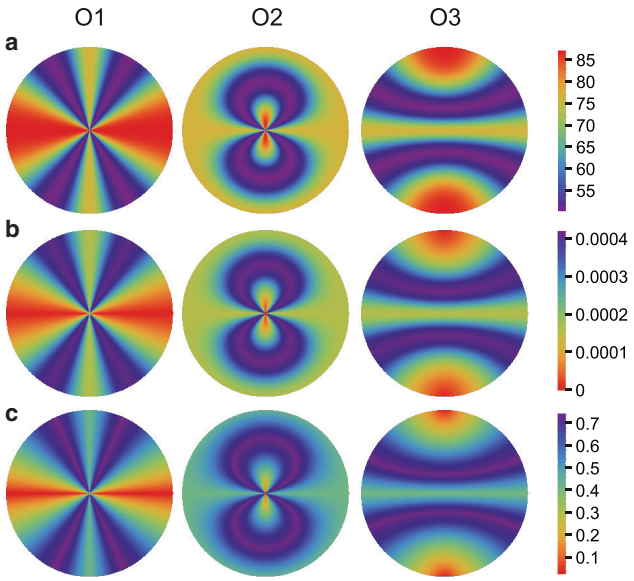

FIGURE 5 Stereographic projections of (*a*) $\varepsilon_H(\nu, \kappa)$, (*b*) the standard deviation of $\Phi_S(\nu, \kappa)$, and (*c*) $A(\nu, \kappa)$ using the default model signal for the three orientations, O1–O3.

them is the result of integrating the information available from each of the cells. Hence, the fact that different radical pair orientations result in different values of ε_H must be reflected at the level of individual receptors. We refer to the ε_H generated by a pattern of r receptors absorbing p photons per receptor as the joint lower bound, and the ε_H generated by any one of the r receptors absorbing rp photons as the individual lower bound, denoted $\varepsilon_H(\nu, \kappa)$. The calculation of $\varepsilon_H(\nu, \kappa)$ for a receptor cell located at position (ν, κ) on the retina can be divided into three steps: 1) find the angle $\zeta(\nu, \kappa)$ between the geomagnetic field and the symmetry axis of the radical pairs bound inside the cell, as a function of the head direction θ, using Eqs. 2, 3, and 4; 2) find the signal $\Phi_S(\nu, \kappa)$ from this cell, again as a function of θ, using Eq. 1; 3) calculate $\varepsilon_H(\nu, \kappa)$ using Eq. 5 with $r = 1$. We now investigate the connections among these steps using the same projection as in Fig. 4 to visualize, initially, $\varepsilon_H(\nu, \kappa)$ instead of $\Phi_S(\nu, \kappa)$.

Starting from step 3 above, Fig. 5 *a* shows the projection of $\varepsilon_H(\nu, \kappa)$ for each of the three orientations with $rp = 3 \times 10^6$. In each case, there is a curve of minimal $\varepsilon_H(\nu, \kappa)$ (*violet*), which is X-shaped for O1, 8-shaped for O2, and $\asymp$-shaped for O3. We shall call this the "minimal curve" on the retina surface. The patterns in Fig. 5 *a* bear a clear resemblance to the corresponding projections of $\Phi_S(\nu, \kappa)$ in the middle row of Fig. 4.

Moving up to step 2, Fig. 5 *b* shows the projections of the standard deviation of $\Phi_S(\nu, \kappa)$ over all head directions. These patterns also closely resemble the corresponding projections in Fig. 5 *a*. In particular, the minimal curves exactly agree (note that the color code in Fig. 5 *b* has been inverted for an easier comparison with Fig. 5 *a*). This means that, somewhat surprisingly, almost all the relational information contained in Fig. 5 *a* is captured by Fig. 5 *b* without having to calculate any $\varepsilon_H(\nu, \kappa)$ values.

One step up further, Fig. 5 *c* (again with an inverted color code) shows the stereographic projections of the function

$$A(\nu, \kappa) = \max_{\theta \in [0,2\pi)} |\cos \zeta(\nu, \kappa)| - \min_{\theta \in [0,2\pi)} |\cos \zeta(\nu, \kappa)|, \quad (10)$$

where $\zeta(\nu, \kappa)$ is the angle between the magnetic field axis and the symmetry axis of the radical pairs in the cell at position (ν, κ) in the retina. All relational information is once again almost completely captured, even without having to calculate $\Phi_S(\nu, \kappa)$. The reason why different orientations lead to different joint lower bounds may therefore be traced back to Eq. 10; the greater the variation in $|\cos\zeta(\nu, \kappa)|$ as the eye scans the horizon, the greater the variation in $\Phi_S(\nu, \kappa)$, and therefore the greater precision with which the geomagnetic field direction can be determined.

A feature of the individual lower bound errors in Fig. 5 *a* is that for all three radical pair orientations, the maximal and minimal values of $\varepsilon_H(\nu, \kappa)$ are the same (87.1 and 50.3°, respectively). The latter corresponds to the minimal curve mentioned above. We therefore wondered whether orientations O2 and O3 are able to generate a smaller joint lower bound because more cells have individual lower bounds close to the minimum. To test this, we defined the essential region for a given radical pair orientation as the region surrounding the minimal curve on the retina surface in which every point has an $\varepsilon_H(\nu, \kappa)$ that differs from the minimal $\varepsilon_H(\nu, \kappa)$ by less than 27.8%. The reason for choosing 27.8% is explained by means of Figs. S4 and S5. The essential regions for the three orientations are shown in Fig. 6. Their relative areas are O1:O2:O3 = 1.0:2.3:1.5, supporting the above conjecture. Table 1 compares

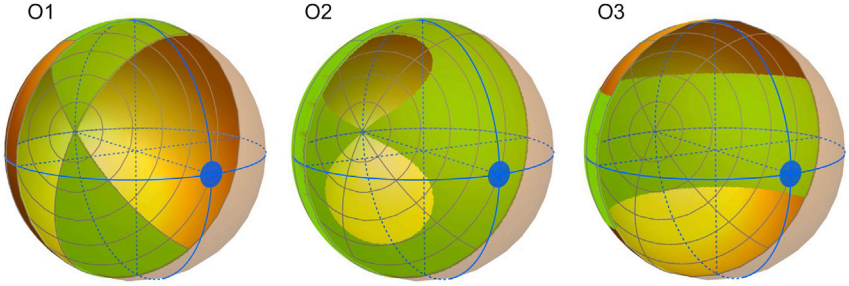

FIGURE 6 Representations of the model eye showing the essential regions (*green*) for the three orientations, O1–O3, superimposed on the retina (*yellow/orange*). The pupil is shown as a blue disk.

TABLE 1 Joint Lower Bounds for Different Distributions of Cells in the Retina

	O1	O2	O3
Whole retina ε_H[a]	12.4°	1.5°	2.6°
Essential region ε_H[b]	4.0°	0.8°	0.6°

Parameters: $a = 0.7$, $b = 0.00381$, $c = 10°$, and $rp = 3 \times 10^6$.
[a]Lower bound error when the receptor cells are uniformly distributed across the whole retina.
[b]Lower bound error when the receptor cells are uniformly distributed in the essential region for each orientation.

values of ε_H for the three orientations with cells distributed uniformly around the retina or with the same number of cells concentrated into the essential region for each orientation. In each case, the latter gives a substantial reduction in ε_H.

Dependence of ε_H on $\Phi_S(\zeta)$

The default parameters of the model signal in Eq. 1 were chosen to provide an approximate match to one particular spin dynamics simulation of a flavin-tryptophan radical pair reaction in cryptochrome (10). For a variety of reasons, the magnetic sensitivity of a cryptochrome magnetic sensor in vivo could be larger or smaller than that given by the default model signal: 1) the radical that partners $FAD^{\bullet-}$ could be magnetically much simpler than $TrpH^{\bullet+}$ (19), 2) the lifetime of the radical pair and its spin coherence could be longer than 1 μs (33), 3) exchange and dipolar interactions should be considered (34), and 4) only half the hyperfine interactions (those with the largest anisotropy) were included in the spin dynamics simulation (20). 1 and 2 would increase the amplitude of the signal, whereas 3 and 4 would reduce it (35). All four would change the width and offset. Presently, there are no experimental data that would provide a better estimate of the signal strength, partly because there have been no measurements of magnetic field effects in vivo and only isotropic effects in vitro (16,17) and partly because a purified cryptochrome (in vitro) is unlikely to have the same behavior in the crowded milieu of a photoreceptor cell, interacting with signaling partners and whatever structures serve to align and immobilize it. It is therefore relevant to explore how ε_H depends on the three parameters in Eq. 1.

Fig. 7, *a–c* show how ε_H for orientation O1 depends on a, b, and c in Eq. 1 for different total number of photons, rp. Relative to the default values, the heading error can be reduced by changing the offset away from 0.5 in either direction (Fig. 7 *a*), by increasing the amplitude of the signal (Fig. 7 *b*), and by reducing its width (Fig. 7 *c*). The dependence on the amplitude, b, is relatively simple; ε_H is a function of b^2rp only (Fig. S6). That is, if the amplitude of the signal is doubled, four times fewer photons in total are required to achieve the same ε_H. Under similar conditions, O2 and O3 exhibit the same kind of dependence on a, b, and c but generally give smaller values of ε_H (as noted above for the default signal).

There is thus considerable scope for optimizing the properties of the radicals and their orientation in the receptor cells to improve the precision of the compass bearing. This point can be illustrated by making stepwise changes in the parameters to reduce the number of photons required to achieve $\varepsilon_H = 5°$. Fig. 8 shows ε_H for six cases (see Table 2) starting with O1 and the default values of a, b, and c and ending at O2 with $a = 0.9$, $b = 0.00508$, and $c = 10°$. Making these relatively modest changes to the model signal and choosing orientation O2 in preference to O1 reduces the total number of photons required for $\varepsilon_H = 5°$ by a factor of almost 600 and reduces the value of ε_H predicted for $rp = 3.94 \times 10^5$ photons from 82.7 to 5° (Table 2). This value of rp is considerably smaller than the estimated number of available photons (3×10^8; see above).

CONCLUSIONS

We have investigated the angular precision of the light-dependent compass sense of night-migratory songbirds using the information theory approach devised by Hiscock et al. (10). To avoid explicit modeling of more than a million receptor cells in the retina, neighboring cells have been grouped together on the basis that they should have a similar

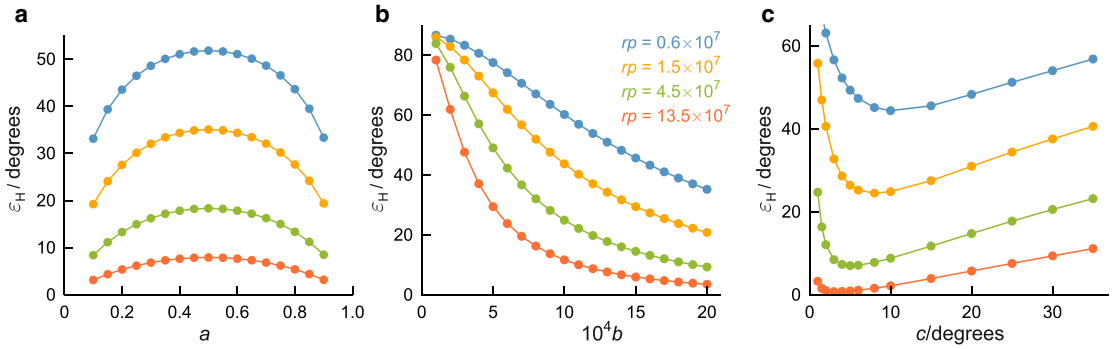

FIGURE 7 (*a*) Dependence of ε_H on a, the offset of $\Phi_S(\zeta)$, is shown: $b = 0.00127$, $c = 26°$. (*b*) Dependence of ε_H on b, the amplitude of $\Phi_S(\zeta)$, is shown: $a = 0.5$, $c = 26°$. (*c*) Dependence of ε_H on c, the width of $\Phi_S(\zeta)$, is shown: $a = 0.5$, $b = 0.00127$. Orientation O1 was used for all three panels.

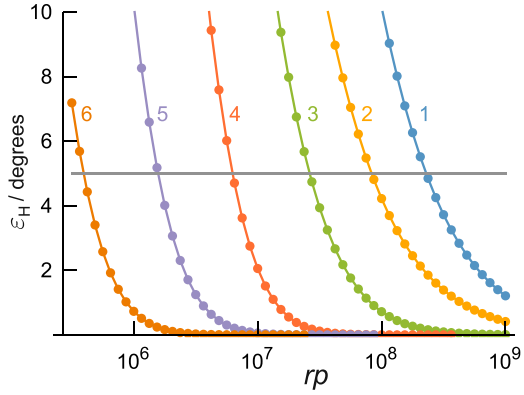

FIGURE 8 Dependence of ε_H on rp for the six sets of parameters in Table 2 showing sequential improvements to the lower bound head direction error. The horizontal line marks $\varepsilon_H = 5°$.

response to the geomagnetic field. This approximation has been validated here by the finding that the lower bound error, ε_H, is independent of the size of these groups provided the total number of photons absorbed in the retina, and therefore radical pairs formed, is fixed (Fig. 2). Doubling the number of groups and halving the number of photons absorbed by each group, for example, has no effect on ε_H. The only restrictions on this finding are that there must be at least 100 groups of cells distributed uniformly around the retina and that the parameters of the model signal in Eq. 1 should not have extreme values.

The conclusion that the total number of photons controls the precision of the compass also has a bearing on a question posed in (5): whether ε_H would be affected by considering the night sky as a collection of bright stars on a dark background rather than a uniform source of dim light. The inference that can be drawn from the results presented here is that as long as one considers the same total photon flux, the compass performance should not change.

In their treatment, Hiscock et al. considered a single intracellular orientation of the magnetoreceptor proteins (O1), chosen for the simplicity of its visual modulation pattern (Fig. 4; (10)). In terms of ε_H, all other magnetoreceptor orientations perform better than O1 and, other things being equal, orientations O2 and O3 are close to optimal (Fig. 3). Given that essentially nothing is known about how cryptochromes might be immobilized and aligned in the retina, the choice of O1 can be seen as completely arbitrary. What our analysis has shown is that the precision of the compass bearing derived from a radical pair sensor can be optimized by adjusting the orientation of the receptor molecules within the cells.

Furthermore, by calculating individual lower bounds, $\varepsilon_H(\nu, \kappa)$, we have been able to shed light on why some receptor orientations are more successful than others and to show that by concentrating cells into the essential region for each orientation, the performance of the compass can be enhanced (Figs. 4, 5, and 6). It is not clear whether this finding has biological significance.

The angular precision of the information available from a radical pair compass sense depends on the quantum yield of the signaling state and how it varies with the direction of the geomagnetic field with respect to the aligned receptor proteins. We have modeled this dependence by means of Eq. 1 using default values of the parameters a, b, and c that give an approximate match to a detailed spin dynamics simulation of the [$FAD^{\bullet-}$ $TrpH^{\bullet+}$] state of cryptochrome (10). Although a certain amount is known about the magnetic sensitivity of this radical pair from spectroscopic measurements on purified cryptochromes (16,17), there is no information on the anisotropy of the magnetic field effect in vivo. It is therefore possible, indeed likely, that the form of Eq. 1 that best describes the behavior in vivo will deviate significantly from the model used here. Figs. 7 and 8 and Table 2 show that there is considerable scope for optimizing ε_H by making relatively modest changes to a, b, and c.

Previous spin dynamics simulations of the magnetic sensitivity of cryptochrome radical pairs have identified a number of ways in which this optimization could be realized. These include 1) a spin coherence lifetime longer than the 1 μs adopted here (36); 2) asymmetric recombination, i.e., different rate constants for the reactions of singlet and triplet radical pairs (37); 3) replacement of the $TrpH^{\bullet+}$ component of the radical pair by a radical with fewer and smaller electron-nuclear hyperfine interactions (19); and 4) modified reaction schemes involving paramagnetic scavengers (38,39). All of these factors have the potential to alter the offset, amplitude, and width of $\Phi_S(\zeta)$ and so reduce the expected error in the derived compass bearing. Conversely, the uncertainty in the head direction can be expected to increase if the amplitude of the signal in vivo is smaller than in the default model.

TABLE 2 Sequential Improvement in ε_H Obtained by Changing the Details of the Model Signal, $\Phi_S(\zeta)$, and the Orientation of the Receptors

	a	b	c	O	$rp/10^5$[a]	rp (rel)[b]	ε_H[c]
1	0.5	0.00127	26°	1	2290	582	82.7°
2	0.9	0.00127	26°	1	831	211	76.2°
3	0.9	0.00127	10°	1	263	67	74.1°
4	0.9	0.00127	10°	2	62.7	16	62.4°
5	0.9	0.00254	10°	2	15.7	4	29.3°
6	0.9	0.00508	10°	2	3.94	1	5.00°

See Fig. 8 for illustration.
[a]Total number of photons required for $\varepsilon_H = 5°$.
[b]Relative number of photons required for $\varepsilon_H = 5°$.
[c]Value of ε_H when $rp = 3.94 \times 10^5$.

SUPPORTING MATERIAL

Supporting Material can be found online at https://doi.org/10.1016/j.bpj.2020.12.023.

AUTHOR CONTRIBUTIONS

P.J.H. conceived and designed the study. Y.R. performed the calculations with advice from H.G.H. All authors discussed the results and conclusions. Y.R. and P.J.H. wrote the manuscript.

ACKNOWLEDGMENTS

We are grateful to the following for financial support: the Air Force Office of Scientific Research (Air Force Materiel Command, USAF award no. FA9550-14-1-0095), the European Research Council (under the European Union's Horizon 2020 research and innovation programme, grant agreement no. 810002, Synergy Grant: *QuantumBirds*), and the Office of Naval Research Global, award no. N62909-19-1-2045.

REFERENCES

1. Wiltschko, W., and R. Wiltschko. 1972. Magnetic compass of European robins. *Science.* 176:62–64.
2. Wiltschko, R., and W. Wiltschko. 1995. Magnetic Orientation in Animals. Springer Verlag, Berlin, Germany.
3. Mouritsen, H. 2018. Long-distance navigation and magnetoreception in migratory animals. *Nature.* 558:50–59.
4. Nordmann, G. C., T. Hochstoeger, and D. A. Keays. 2017. Magnetoreception-A sense without a receptor. *PLoS Biol.* 15:e2003234.
5. Hore, P. J., and H. Mouritsen. 2016. The radical-pair mechanism of magnetoreception. *Annu. Rev. Biophys.* 45:299–344.
6. Ritz, T., S. Adem, and K. Schulten. 2000. A model for photoreceptor-based magnetoreception in birds. *Biophys. J.* 78:707–718.
7. Zapka, M., D. Heyers, …, H. Mouritsen. 2009. Visual but not trigeminal mediation of magnetic compass information in a migratory bird. *Nature.* 461:1274–1277.
8. Wiltschko, W., and R. Wiltschko. 2001. Light-dependent magnetoreception in birds: the behaviour of European robins, *Erithacus rubecula*, under monochromatic light of various wavelengths and intensities. *J. Exp. Biol.* 204:3295–3302.
9. Wiltschko, R., K. Stapput, …, W. Wiltschko. 2010. Directional orientation of birds by the magnetic field under different light conditions. *J. R. Soc. Interface.* 7 (*Suppl 2*):S163–S177.
10. Hiscock, H. G., T. W. Hiscock, …, P. J. Hore. 2019. Navigating at night: fundamental limits on the sensitivity of radical pair magnetoreception under dim light. *Q. Rev. Biophys.* 52:e9.
11. Cochran, W. W., H. Mouritsen, and M. Wikelski. 2004. Migrating songbirds recalibrate their magnetic compass daily from twilight cues. *Science.* 304:405–408.
12. Lau, J. C. S., C. T. Rodgers, and P. J. Hore. 2012. Compass magnetoreception in birds arising from photo-induced radical pairs in rotationally disordered cryptochromes. *J. R. Soc. Interface.* 9:3329–3337.
13. Worster, S., H. Mouritsen, and P. J. Hore. 2017. A light-dependent magnetoreception mechanism insensitive to light intensity and polarization. *J. R. Soc. Interface.* 14:20170405.
14. Wolfram Research Inc. 2020. Wolfram Mathematica 12.
15. Wu, H., A. Scholten, …, K. W. Koch. 2020. Protein-protein interaction of the putative magnetoreceptor cryptochrome 4 expressed in the avian retina. *Sci. Rep.* 10:7364.
16. Maeda, K., A. J. Robinson, …, P. J. Hore. 2012. Magnetically sensitive light-induced reactions in cryptochrome are consistent with its proposed role as a magnetoreceptor. *Proc. Natl. Acad. Sci. USA.* 109:4774–4779.
17. Sheppard, D. M. W., J. Li, …, S. R. Mackenzie. 2017. Millitesla magnetic field effects on the photocycle of an animal cryptochrome. *Sci. Rep.* 7:42228.
18. Cintolesi, F., T. Ritz, …, P. J. Hore. 2003. Anisotropic recombination of an immobilized photoinduced radical pair in a 50-μT magnetic field: a model avian photomagnetoreceptor. *Chem. Phys.* 294:385–399.
19. Lee, A. A., J. C. S. Lau, …, P. J. Hore. 2014. Alternative radical pairs for cryptochrome-based magnetoreception. *J. R. Soc. Interface.* 11:20131063.
20. Lewis, A. 2018. Spin Dynamics in Radical Pairs. Springer International Publishing, Cham, Switzerland.
21. Lestas, I., G. Vinnicombe, and J. Paulsson. 2010. Fundamental limits on the suppression of molecular fluctuations. *Nature.* 467:174–178.
22. Hilfinger, A., T. M. Norman, …, J. Paulsson. 2016. Constraints on fluctuations in sparsely characterized biological systems. *Phys. Rev. Lett.* 116:058101.
23. Shannon, C. E. 1948. A mathematical theory of communication. *Bell Syst. Tech. J.* 27:379–423.
24. Jaynes, E. T. 1957. Information theory and statistical mechanics. *Phys. Rev.* 106:620–630.
25. Ihara, S. 1993. Information Theory for Continuous Systems. World Scientific, Singapore.
26. Cover, T. M., and J. A. Thomas. 2012. Elements of Information Theory. John Wiley & Sons, Hoboken, NJ.
27. Beaudry, N. J., and R. Renner. 2011. An intuitive proof of the data processing inequality. *arXiv*, arXiv:1107.0740 https://arxiv.org/abs/1107.0740.
28. Nielsen, M. A., and I. L. Chuang. 2010. Quantum Computation and Quantum Information. Cambridge University Press, New York.
29. Akesson, S., J. Morin, …, U. Ottosson. 2001. Avian orientation at steep angles of inclination: experiments with migratory white-crowned sparrows at the magnetic North Pole. *Proc. Biol. Sci.* 268:1907–1913.
30. Lefeldt, N., D. Dreyer, …, H. Mouritsen. 2015. Migratory blackcaps tested in Emlen funnels can orient at 85 degrees but not at 88 degrees magnetic inclination. *J. Exp. Biol.* 218:206–211.
31. Kram, Y. A., S. Mantey, and J. C. Corbo. 2010. Avian cone photoreceptors tile the retina as five independent, self-organizing mosaics. *PLoS One.* 5:e8992.
32. Thomas, R. J., T. Székely, …, P. D. Wallis. 2002. Eye size in birds and the timing of song at dawn. *Proc. Biol. Sci.* 269:831–837.
33. Kobylkov, D., J. Wynn, …, H. Mouritsen. 2019. Electromagnetic 0.1-100 kHz noise does not disrupt orientation in a night-migrating songbird implying a spin coherence lifetime of less than 10 μs. *J. R. Soc. Interface.* 16:20190716.
34. Efimova, O., and P. J. Hore. 2008. Role of exchange and dipolar interactions in the radical pair model of the avian magnetic compass. *Biophys. J.* 94:1565–1574.
35. Hore, P. J. 2019. Upper bound on the biological effects of 50/60 Hz magnetic fields mediated by radical pairs. *eLife.* 8:e44179.
36. Hiscock, H. G., S. Worster, …, P. J. Hore. 2016. The quantum needle of the avian magnetic compass. *Proc. Natl. Acad. Sci. USA.* 113:4634–4639.
37. Lewis, A. M., D. E. Manolopoulos, and P. J. Hore. 2014. Asymmetric recombination and electron spin relaxation in the semiclassical theory of radical pair reactions. *J. Chem. Phys.* 141:044111.
38. Kattnig, D. R., and P. J. Hore. 2017. The sensitivity of a radical pair compass magnetoreceptor can be significantly amplified by radical scavengers. *Sci. Rep.* 7:11640.
39. Kattnig, D. R. 2017. Radical-pair-based magnetoreception amplified by radical scavenging: resilience to spin relaxation. *J. Phys. Chem. B.* 121:10215–10227.